

Six-stage cascade paramagnetic mode magnetophoretic separation system for human blood samples

Youngdo Jung · Yoonsu Choi · Ki-Ho Han ·
A. Bruno Frazier

Published online: 28 March 2010
© Springer Science+Business Media, LLC 2010

Abstract This paper is focused on the development of a six-stage cascade paramagnetic mode magnetophoretic separation (PMMS) system for separating suspended cells in blood based on their native magnetic properties. The design and fabrication of a PMMS system are presented and the microfluidic separation system is characterized experimentally using human whole blood as the case study. The PMMS system can separate blood cells types continuously using the magnetophoretic force produced from a high magnetic field gradient without magnetic or fluorescent tagging. Experimental results demonstrated that red blood cell separation in the PMMS system at a volumetric flow rate of 28.8 $\mu\text{L} / \text{hr}$, resulting in a separation time of 10.4 min for a 5.0 μL blood sample with a separation efficiency of 89.5 \pm 0.20%. The PMMS system was tested at higher volumetric flow rates of 50.4 $\mu\text{L} / \text{hr}$ and 72.0 $\mu\text{L} / \text{hr}$. The measured separation efficiencies were 86.2 \pm 1.60% and 59.9 \pm 6.06% respectively.

Keywords Human whole blood · Cell separator · High Gradient Magnetic Field Separation (HGMS) · Magnetophoresis · Microfluidic system

1 Introduction

This work presents the design, fabrication and experimental characterization of a six-stage cascade paramagnetic mode magnetophoretic separation system using human whole blood as the case study.

The ability to manipulate suspended biological cells is fundamental to medical research and clinical applications. Examples of applications include concentration of sparse cancer cells from low density suspensions, preparation of cell-free plasma or serum samples from whole blood, and genetic analysis from white blood cells in blood samples.

One of most widely used macro systems for cell separation and collection is fluorescence activated cell sorting (FACS) based on immuno-fluorescence. FACS can separate many types of cells with high efficiency using fluorescent tags (Herzenberg et al. 2002). Magnetically-activated cell separation (MACS) provides a gentler and faster enrichment technology by labeling cells with magnetic beads and separating them using magnetic forces (Thiel et al. 1998). Despite their high separation and enrichment efficiency, FACS and MACS have several drawbacks including a relatively large minimum sample size, the need for labeling the samples using fluorescent and magnetic tags, and expensive equipment. Density gradient centrifugation provides a cheaper and easier alternative. However, it is a discontinuous batch process and requires additional steps for down stream cell manipulation and collection. Filtration through micro-pores is an easily accessible option in separating cells using size differences, but clogging problem makes it only suitable for batch type separations.

Microfluidic cell separation systems are of great interest because of the ability to create very strong forces over distances on the same geometrical scale as most biological

Y. Jung · Y. Choi · A. B. Frazier (✉)
School of Electrical and Computer Engineering,
Georgia Institute of Technology,
777 Atlantic Drive,
Atlanta, GA 30332-0250, USA
e-mail: Bruno.Frazier@ece.gatech.edu

K.-H. Han
School of Nano Engineering, Inje University,
607 Obang-dong,
Gimhae, Gyongnam 621-749, Republic of Korea

cells of interest (Toner and Irimia 2005). Also, these microsystems generally exhibit shorter processing times, less operational costs, the potential to be used as a point-of-care device due to their compact size, and the potential to be integrated with additional analytical functions to realize complex analytical systems in micro device format. Various microfluidic systems have been developed for separating cells based on size differences (Yamada and Seki 2006; Vankrunkelsven et al. 2004; Chen et al. 2008; Choi and Park 2007; Maenaka et al. 2008), intrinsic dielectric affinity differentiation (Gascoyne and Vykoukal 2002; Becker et al. 1995; Han and Frazier 2008; Pommer et al. 2008; Cheng et al. 2007), and optical interaction (Applegate et al. 2004; Dholakia et al. 2007; MacDonald et al. 2003, 2004; Sun et al. 2007; Wang et al. 2005; Ozkan et al. 2003).

Separating target cells other than RBCs in the whole blood without microenvironment alteration has been a challenge for integrated microsystem for several reasons including the complexity of the fluid and the density of the cells. Human whole blood consists of 45% blood cells and 55% plasma with 98% of the blood cells being red blood cells (RBCs) with a cell density of around 5×10^6 cells / μL . Therefore, using whole blood as an input sample requires the integration of essential functionalities such as purification, washing, and extraction technologies in order to achieve most blood-based analytical goals.

High gradient magnetic field separation (HGMS) has been shown to be an effective method for removal of metal or radioactive particles from waste fluid and gases in many macro scale industrial applications (Ebner et al. 1999; Kakihara et al. 2004; Ngomsik et al. 2005; Sarikaya et al. 2006). Additionally, HGMS has been applied to biological applications, such as purification of proteins (Ditsch et al. 2006), extracting synthesized organic compounds from water (Moeser et al. 2002) and locally targeted drug delivery (Chen et al. 2004; Ritter et al. 2004; Yellen et al. 2005). Various cell sorting or extraction systems using HGMS have been successfully demonstrated in macroscale systems (Miltenyi et al. 1990; Thomas et al. 1992; Richards et al. 1996) and in microscale systems (Pamme and Wilhelm 2006; Pamme et al. 2006; Schneider et al. 2006; Adams et al. 2008). However, the above mentioned biological applications require magnetic tagging of the cells and molecules in order to produce enough force for the systems to achieve effective separations.

It has been reported that in whole blood, deoxyhemoglobin RBCs show a much higher magnetic susceptibility than other biological cells and can be treated as paramagnetic particles, while white blood cells (WBCs) behave like diamagnetic particles (Melville et al. 1975). Using their native magnetic properties, deoxyhemoglobin RBCs have been manipulated in macroscale HGMS devices (Melville et al. 1975; Takayasu et al. 2000; Zborowski et al. 2003). Microscale

HGMS devices have the advantage of producing much higher magnetic field gradients in the proximity of microscopic magnetic structures (Toner and Irimia 2005), thus RBCs, WBCs and other rare circulating cells (e.g. circulating tumor cells) can be separated more successfully (Xia et al. 2006; Han and Frazier 2005a, 2006a).

Previously proposed paramagnetic microsystems for blood cells separation (Han and Frazier 2006b) have shown high separation efficiency of 93.5% for RBCs and 97.4% for WBCs at a volumetric flow rate of 5 μL / hr corresponding to 2.5×10^6 cells / hr. However, the separation efficiencies decreased to 75% and 65% as the volumetric flow rate increased to 20 μL / hr and 30 μL / hr, which hindered its application to fast processing of small volumes of blood sample ($\sim 5 \mu\text{L}$) from the finger tip or a cotton swab, etc. The six stage cascade PMMS system discussed in this work can separate RBCs from human whole blood sample continuously with minimal damage to the cellular components of blood with a separation throughput of 28.8 μL / hr and 50.4 μL / hr. Experimental results show a separation efficiency of $89.5 \pm 0.20\%$ and $86.2 \pm 1.60\%$ for red blood cells respectively.

This paper presents the design, fabrication steps and experimental setup of a six stage PMMS system. Quantitative measurements of RBC separation efficiencies using the six stage cascade PMMS system are reported for various flow rates.

2 Method

2.1 Design

A cross sectional schematic of the PMMS system is shown in Fig. 1. A uniform external magnetic field generated by

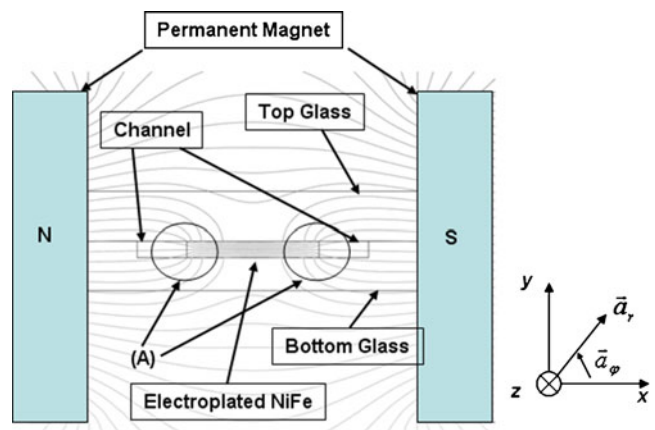


Fig. 1 A high magnetic field gradient is generated in the region (A) around ferromagnetic structures using permanent magnets as the field source. The RBCs are attracted toward the ferromagnetic capture structure by the paramagnetic force created by the gradient

an external permanent magnet is deflected around the ferromagnetic structures, and a high gradient magnetic field is created near the ferromagnetic structures. In a high gradient magnetic field, blood cells experience an attractive or repulsive magnetophoretic force depending on their native magnetic properties. The magnetic force, F_{BC} , on a blood cell based in our previous work (Han and Frazier 2004) can be expressed as

$$\begin{aligned} \vec{F}_{BC} = & -\frac{2\kappa\mu_o\Delta\chi V_{BC}a^2}{r^3} \left[\kappa\left(\frac{w}{h}\right)\frac{a^2}{r^2} + \cos(2\phi) \right] \\ & \times \left(\frac{w}{h}\right)H_o^2\vec{a}_r - \frac{2\kappa\mu_o\Delta\chi V_{BC}a^2}{r^3} \sin(2\phi) \\ & \times \left(\frac{w}{h}\right)H_o^2\vec{a}_\phi, r > a \\ \left(\kappa = \frac{\mu_w - \mu_B}{\mu_w + \mu_B} \right) \end{aligned} \tag{1}$$

where μ_o , μ_B and μ_w are the magnetic susceptibilities of the air, the buffer solution, and the ferromagnetic structures, respectively; H_o is the external magnetic field; χ_{BC} and χ_B are the magnetic susceptibilities of the blood cell and the buffer solution; $\Delta\chi$ ($= \chi_{BC}-\chi_B$) is the relative magnetic susceptibility of a blood cell with respect to the buffer solution; V_{BC} is the volume of the blood cell; a is the radius of the circular ferromagnetic wire, which is half of rectangular wire’s height; w and h are the width and height

of rectangular wire; r and ϕ are the cylindrical coordinates of the distance and angle; and \vec{a}_r and \vec{a}_ϕ are unit vectors for the distance and angle in the cylindrical coordinate, respectively.

From Eq. 1, when magnetic particles are placed on the x-axis or in the microfluidic channel in Fig. 1 ($\phi \approx 0^\circ$ or 180° , $\sin 2\phi \approx 0$, $\cos 2\phi \approx 1$), magnetic particles whose $\Delta\chi$ is positive (paramagnetic particles) are attracted toward the ferromagnetic structures, while those that have negative $\Delta\chi$ are pushed away from the ferromagnetic structures. Deoxyhemoglobin RBCs have a positive $\Delta\chi$ in most buffer solutions and are thusly attracted toward the ferromagnetic capture structure by the paramagnetic force (Han and Frazier 2006a).

Previously proposed paramagnetic microsystems for blood cells separation have shown high separation efficiency of 93.5% for RBCs and 97.4% for WBCs at a volumetric flow rate of 5.0 $\mu\text{L} / \text{hr}$, but suffered a drastic drop in the separation efficiencies as the volumetric flow rate was increased to 20 $\mu\text{L} / \text{hr}$ and 30 $\mu\text{L} / \text{hr}$. To increase the volumetric flow rate while maintaining high separation efficiency, this work presents a new magnetophoretic microseparation system design to introduce several changes. One of the most important factors considered in the design of six stage magnetophoretic separation system was the required trapping time for the RBCs to move from position (x_1, y) to position (x_2, y) , $x_1 \geq x_2$. In our previous work (Han and Frazier 2006b), the trapping time was calculated as

$$\begin{aligned} t = & \frac{3\mu_o\eta(A/l)}{\Delta\chi V_{BC}(\mu_o M_S)B_o a^2} \\ & \times \left[(x_1^4 - x_2^4) + 2(6y^2 - Ka^2)(x_1^2 - x_2^2) + 2(K^2a^4 + 21y^4 - 9Ka^2y^2) \times \ln\left(\frac{x_1^2 + Ka^2 - 3y^2}{x_2^2 + Ka^2 - 3y^2}\right) + \frac{2y^6}{3y^2 - Ka^2} \ln\left(\frac{x_2^2}{x_1^2} \times \frac{x_1^2 + Ka^2 - 3y^2}{x_2^2 + Ka^2 - 3y^2}\right) \right], \\ K = & \frac{\mu_o M_S}{2B_o} \end{aligned} \tag{2}$$

where η is the apparent viscosity of the blood cells in the buffer solution; A is the maximum cross-section area presented perpendicular to the velocity; l is the characteristic length of the blood cell in the direction of velocity vector; M_S is the saturation magnetization field of the rectangular wire; and B_o is the external magnetic flux.

One design option was to increase the number of separation stages. By increasing the number of separation stages, already captured RBCs would be swept into the center collection channel providing more space for other RBCs to be attracted to the ferromagnetic structures consequently increasing the separation efficiency. Also if the size of glass slide containing the microseparation system is limited and the diagonal collection channels are saturated with separated RBCs, increasing the number of

separation stages in the design consequently increases the number of diagonal collection channels and the total volume of collected RBCs. Thus, to achieve similar separation efficiency, the required effective trapping time could be decreased. However, the number of separation stages can not be increased indefinitely. To move RBCs from one point in the outer feed channels to a point in the outer channels where the cells can be swept into diagonal collection channels, the RBCs need to be exposed to the lateral magnetophoretic forces for at least a minimum critical amount of time as described in Eq. 2. Shortening the length of each stage reduces the collection time for RBCs in the main, outer separation channels. The minimum design length for each stage has been chosen long enough so that the residence time of the RBCs at each stage was greater

than the minimum capture time at a given volumetric flow rate. In this work, the total length of main separation chamber was chosen to be 48 mm. For the cells to pass through the separation chamber within 5 min, the average flow velocity should be higher than 0.16 mm/s. To achieve the volumetric flow rate of 20 $\mu\text{L/hr}$ or higher with the fore-mentioned minimum flow velocity and 5 min analysis time, the cross sectional area of each of the two main channels should be approximately $1.74 \times 10^4 \mu\text{m}^2$ or larger, and is decided as $2.0 \times 10^4 \mu\text{m}^2$. The channel depth was chosen to be 100 μm considering the available fabrication process. The required trapping time for RBCs was calculated to be approximately 35 s. Considering the trapping time, the minimum average flow rate, and the channel dimensions, each separation stage should be 5.6 mm or longer length. The actual length of separation stage was chosen to be 8.0 mm, thus the number of separation stages was increased to six.

The second design option was increasing the cross sectional area of the separation channels. In the previous paragraph, the microchannel depth was increased from 50 μm to 100 μm . Moreover, to achieve the minimum cross sectional area of $2.0 \times 10^4 \mu\text{m}^2$, the channel width was increased to 200 μm . However, those cells initially positioned 100 μm or greater away from the ferromagnetic structures would be hard to capture efficiently. To overcome this limitation, the channel width of first separation stage was chosen to be 200 μm , but in subsequent separation stages, the width was decreased down to 180 μm , 160 μm , 140 μm , 120 μm , 100 μm , and 100 μm by designing the width of ferromagnetic structures wider.

As shown in Fig. 2, the whole blood sample entered the PMMS system and was subsequently split evenly between the two outer separation microchannels flowing parallel to the ferromagnetic structures. The RBCs were attracted to the ferromagnetic structures by the force produced by the magnetic field gradient and forced into the center microchannel through the diagonal collection channels, while WBCs and other rare cells were forced outward and travel

along the two outer channels. The fluid channel network was designed so that only the RBCs forced to the edge of the ferromagnetic capture structure were swept into the diagonal collection channels, while other cells in the flow stream had a low probability of being swept into the collection channels. The remaining RBCs in the outer channels were attracted and separated into the center flow channel at the subsequent separation stages. By combining six separation stages in a cascade mode, the RBC level in the outer channel was reduced stage by stage and after six separation stages, the RBCs were removed from the flow stream in the two outer channels (Fig. 2).

2.2 Fabrication

The PMMS system consisted of microfluidic channels, ferromagnetic structures, microfluidic interconnections, and the supporting packaging. In the fabrication of the separation system, a 500 \AA chromium layer and a 2000 \AA gold layer were sputtered on both sides of a Schott Borofloat glass substrate (SB-1, S. I. Howard Glass Co., Inc., Worcester, MA, USA) using a Unifilm DC sputter (PVD-300, Unifilm Technology, LLC., Boulder, CO, USA). Positive photoresist was spin-coated at 5,000 rpm for 30 s on the front-side of the glass substrate and soft baked in a vacuum oven at 120°C for 1 min. The microfluidic channel was patterned through ultraviolet (UV) light exposure using the OAI Mask Aligner (Optical Associates, Inc., San Jose, CA, USA) and developed. The back side and perimeter edges of the substrate were coated with positive photoresist and hard baked in a vacuum oven at 120°C for 5 min. The exposed Cr/Au layers on the front side were subsequently etched in Cr and Au etchant, and a 100 μm deep microchannel was realized by wet etching of the glass for 1 h in 49% hydrofluoric acid diluted 3:3:1 using deionized water and nitric acid (Fig. 3(a)). After removing the photoresist and metal masking layers, 150 \AA , 1500 \AA , and 1000 \AA titanium/copper/chromium electroplating seed layers were sputtered over the surface of the

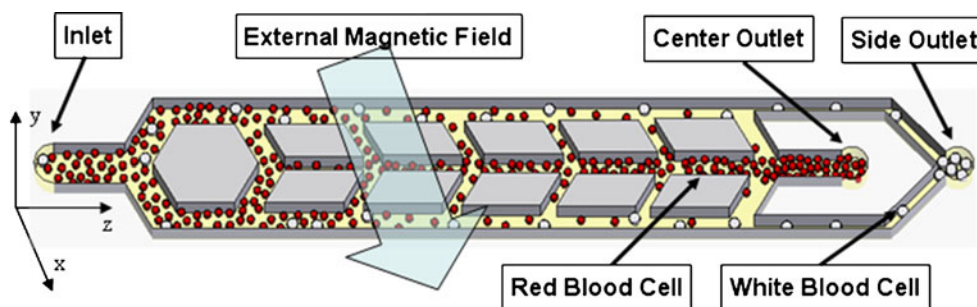


Fig. 2 Operation of the PMMS system: The RBCs are attracted to the ferromagnetic structure and forced into the center channel, while WBCs and other rare cells are forced outward and travel

along the two outer channels. The remaining RBCs in the outer channel are attracted and separated again subsequent separation stages

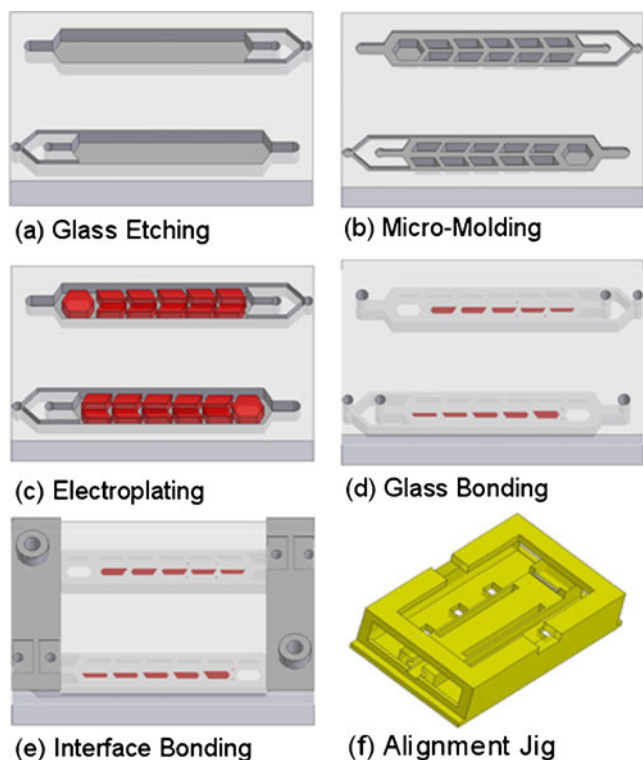


Fig. 3 The fabrication process for the six-stage cascade PMMS system

etched glass substrate using the Unifilm DC sputter. Thick photoresist was spin coated at 300 rpm over the surface of the etched glass substrate, resulting in a measured thickness of photoresist over the 100 μm deep microchannel area of 130 μm. The substrate with uncured photoresist on the top surface was planarized by leaving it on a flat, level surface for 30 min before soft baking. Afterwards, the substrate was soft baked on a hot plate at 110°C for 20 min. The ferromagnetic capture structure electroplating molds were patterned by UV light exposure using the Karl Suss MA-6 Mask Aligner (Karl Suss America, Inc., Waterbury Center, VT, USA) and development in photoresist developer (Fig. 3(b)). The ferromagnetic capture structures located within the patterned flow channel, 100 μm thick, were realized by electroplating NiFe permalloy using a Ni₈₁Fe₁₉ electroplating bath (Frazier 1993) on the pre-defined seed layer after removing the exposed Cr layer. The electroplating process was carried out at room temperature with a current density of 20 mA / cm². Following the electroplating process, the thick photoresist molds and seed layers were removed by chemical etching, resulting in the patterned ferromagnetic structures within the microfluidic channel network (Fig. 3(c)).

A Viper™ SLA® stereolithography system (3D Systems, Co., Rock hill, SC, USA) was used to fabricate a drilling guide to enable correct positioning of the inlet and outlet ports in the top glass. The inlet and outlet holes were defined in the blank top glass using a 1.0 mm diameter

diamond drill bit for drilling. In earlier work, the drilled top glass was aligned and thermally bonded with the patterned bottom glass in a box furnace at 685°C for 3.5 h in a nitrogen gas environment (Fig. 3(d)). The Curie temperature of Ni₈₁Fe₁₉ alloy powder is 567°C and the thermal bonding process at 685°C is known to decrease the permeability of Ni₈₁Fe₁₉ alloy (Colling 1969). Therefore in these studies, the top and bottom glasses were aligned and bonded using UV curable adhesive resin (Renshape® SL 5510, Vantico A&T US, Inc. Lansing, MI, USA)

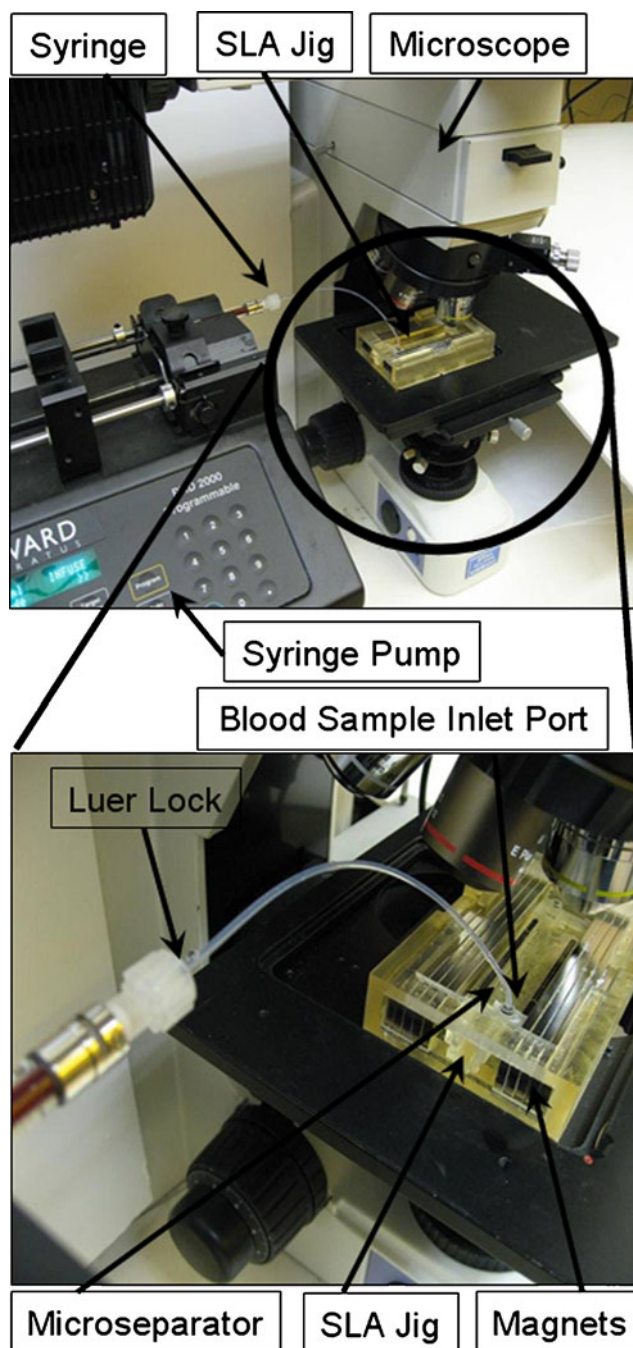


Fig. 4 Instrument set-up for testing the PMMS system

applied between the two glasses by capillary force and cured under a UV lamp for 30 min.

A microfluidic interface was fabricated using the Viper™ SLA® system. The microfluidic interface included fluid interconnects for connecting external tubing, and an o-ring was added to provide reliable, leak-free fluid interconnection and sealing between the microsystem and the external capillary tubing (Han and Frazier 2005b). Finally, the SLA-based microfluidic interface was bonded to the microseparator chip using UV curable resin (Renshape® SL 5510, Vantico A&T US, Inc. Lansing, MI, USA) between the microsystem and the interface. The resin was cured using UV light exposure for 30 min (Fig. 3 (e)). A jig was fabricated using stereolithography to enable proper alignment of the external magnetics to the microseparation system, Fig. 3(f). The alignment jig was

composed of two side pockets to hold the permanent magnets and one center cavity to hold the assembled microsystem.

2.3 Experimental setup

Human venous blood was collected at the on-campus health center under an Institutional Review Board-approved protocol for blood collection for research purposes. The samples were drawn into evacuated glass tubes, containing ethylenediamine tetraacetic acid (EDTA) as an anticoagulant. A 3.0 mM deoxidizing isotonic solution was prepared by dissolving sodium hydrosulfite (Sigma-Aldrich Co., St. Louis, Mo, USA) in a calcium and magnesium free phosphate-buffered saline (PBS) solution (Mediatech, Inc., Herndon, VA, USA) at room temperature. The deoxidiza-

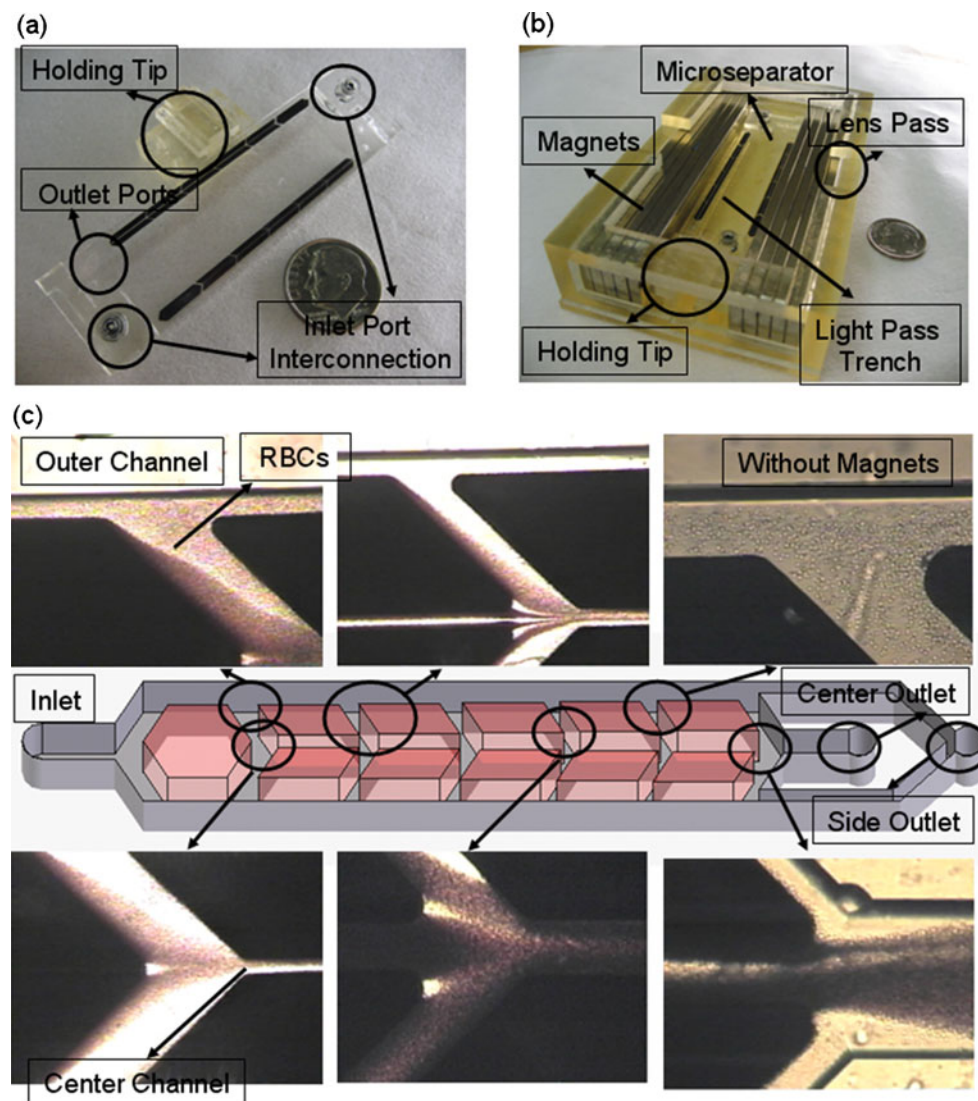


Fig. 5 The fabricated PMMS system (a), package (b), and Micrographs of the blood cell separation at each stage (c)

tion and dilution of the blood sample were achieved by adding 500 μL of the 3 mM isotonic sodium sulfite solution to 50 μL of whole blood. SYTO-13 fluorescent dye was used to identify the nucleated cells during experiments. The blood sample with SYTO-13 fluorescent dye was incubated for 1 h.

Before introducing the sample, the PMMS system was first treated with Pluronic[®] F108 tri-block copolymer surfactant (BASF Co., Florham Park, NJ, USA) solution to reduce the adhesion of blood cells on the channel surfaces. After treating the glass surfaces, the substrates were subsequently washed several times with PBS solution.

The fabricated device was mounted onto the center cavity inside the SLA alignment jig and permanent magnets were inserted into the side pockets to create an external magnetic flux. A 500 μL gas tight glass syringe (Hamilton Co., Reno, NV, USA) was used to load the incubated blood sample and connected to capillary tubing through Luer-tight[™] fitting (Upchurch Scientific, Inc., Oak Harbor, WA, USA). The other end of tubing was connected to the device inlet port through the SLA microfluidic interface. A PHD 2000 syringe pump (Harvard Apparatus, Holliston, MA, USA) was used to provide the desired constant volumetric flow rates during the separation process. The assembled microsystem was placed under a fluorescent microscope and the trajectory of blood cells under a high magnetic gradient flux was monitored using the microscope camera and video capture tools (Fig. 4). 2.5 μL of fluid was collected at each outlet port using adjustable pipettes (Series 2000, Eppendorf North America Inc., Westbury, NY, USA). The separation efficiency of the PMMS system was characterized by counting the RBCs in the fluid collected at each outlet port using a Coulter cell counter

(Z1 Coulter Particle Counter, Beckman Coulter, Inc., Fullerton, CA, USA).

3 Results

The fabricated six-stage cascade PMMS system is shown in Fig. 5(a). The 100 μm tall ferromagnetic structures inside the microchannel can be seen. The separation systems were fabricated at the perimeter of glass substrates to minimize the distance between the separation channel and the permanent magnets and thusly maximize the magnetic field gradient and magnetophoretic force on the untagged blood cells. The inlet holes were placed away from main channel to give more room for microscope lens movement above the separation chamber during the experiments. The outlet holes remained open to air to collect the separated blood samples with the adjustable pipettes. A holding tip was used in the removable part of the alignment jig to hold the microsystem during the experiments.

Figure 5(b) shows the PMMS system packaged inside the alignment jig with the permanent magnets in the side pockets. The alignment jig was designed such that the permanent magnets could be positioned to create a magnetic field perpendicular to the sample flow inside the microseparator. The removable holding tip was used for easier installation and removal of the microseparator chip between experiments. Open cavities in the alignment jig under the microchannel area were used to enable monitoring of the blood cell movement during separation by providing light passage from the bottom-side microscope light source.

The separation efficiency of the microsystem was characterized by counting the RBCs in 2.5 μL of the fluid

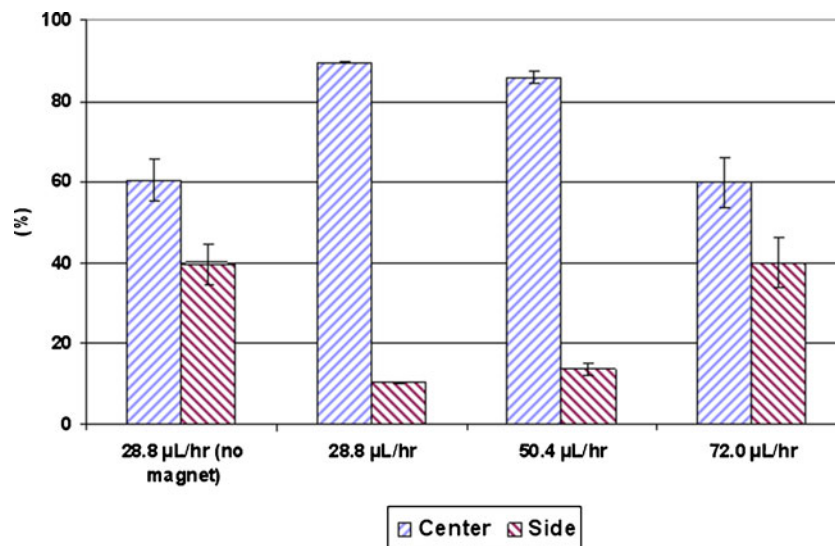


Fig. 6 Measured separation efficiency of RBCs at each outlet for two volumetric flow rates

collected at each outlet port using a Coulter cell counter (Z1 Coulter Particle Counter, Beckman Coulter, Inc., Fullerton, CA, USA). The PMMS system was first tested with a prepared blood sample without an applied magnetophoretic force acting on blood cells by removing the permanent magnets from the package. At the flow rate of 28.8 $\mu\text{L} / \text{hr}$, 60.4 \pm 5.25% of blood cells were collected into the center channel. Figure 5(c) shows images of the RBC separation inside the microchannel at an average flow rate of 28.8 $\mu\text{L} / \text{hr}$ with permanent magnets placed in the side pockets. As the blood sample traveled the length of the microseparator, the RBC level in the outer channels decreased, while the number of RBCs in the center channel increased after each stage. At the output of the central channel in the microseparator, the separation efficiency was measured to be 89.5 \pm 0.20% for RBCs. The PMMS system was tested at higher volumetric flow rates of 50.4 $\mu\text{L} / \text{hr}$ and 72.0 $\mu\text{L} / \text{hr}$. The measured separation efficiencies were lowered to 86.2 \pm 1.60% and 59.9 \pm 6.06% respectively. As the whole blood traveled at a higher flow rate, the residence time of blood cells inside the magnetic field gradient decreased, while the drag force by the flow increased. Thus, the chance for RBCs to be captured into the center channel was reduced (Fig. 6). No clogging due to cell coagulation inside the channel was observed during the separation. However, trapped air bubbles in the channel introduced between experiments blocked the microchannel and prevented further characterization if not removed before starting the separation process.

4 Discussion

The six-stage cascade paramagnetic mode magnetophoretic microseparator was successfully demonstrated for the separation of RBCs from whole blood based on the native magnetic properties without the need for magnetic or fluorescent tagging of the blood sample. Permanent magnets were used to generate an external magnetic field and a high magnetic field gradient around the ferromagnetic structures, enabling a portable hand-held size device. Using a six-stage cascade design, the volumetric sample throughput was increased over previously reported designs to 50.4 $\mu\text{L} / \text{hr}$, which resulted in a processing time of 6.0 min for a 5.0 μL blood sample. With the increased throughput in separating blood cells in a continuous fashion, the presented microsystem can enable fast processing of small volumes of blood sample (\sim 5 μL). The presented microseparator combined further with miniaturized downstream cell sub-classification, detection and analysis systems has the potential to enable high-throughput and efficient blood cell separation and identification as well as to contribute to the development of clinical point-of-care devices for abnormal cell isolation, analysis, and treatment.

Acknowledgements This work was supported by the National Institutes of Health (NIH) under Grant Number ES10846.

Authorships Contributions: Youngdo Jung designed the research, carried out fabrication and experiments, analyzed data, and wrote the paper. Yoonsu Choi carried out fabrication. Ki-Ho Han provided theoretical background for the research. A. Bruno Frazier managed overall research and edited the paper.

Conflict-of-interest disclosure The authors declare no competing financial interests.

References

- J.D. Adams, U. Kim, H.T. Soh, Multitarget magnetic activated cell sorter. *Proc. Natl. Acad. Sci. U.S.A.* **105**, 18165–18170 (2008)
- R.W. Applegate, J. Squier, T. Vestad, J. Oakey, D.W.M. Marr, Optical trapping, manipulation, and sorting of cells and colloids in microfluidic systems with diode laser bars. *Opt. Express* **12**, 4390–4398 (2004)
- F.F. Becker, X.B. Wang, Y. Huang, R. Pethig, J. Vykoukal, P.R.C. Gascoyne, Separation of human breast-cancer cells from blood by differential dielectric affinity. *Proc. Natl. Acad. Sci. U.S.A.* **92**, 860–864 (1995)
- H.T. Chen, A.D. Ebner, A.J. Rosengart, M.D. Kaminski, J.A. Ritter, Analysis of magnetic drug carrier particle capture by a magnetizable intravascular stent: 1. Parametric study with single wire correlation. *J. Magn. Mater.* **284**, 181–194 (2004)
- X. Chen, D.F. Cui, C.C. Liu, H. Li, Microfluidic chip for blood cell separation and collection based on crossflow filtration. *Sens. Actuators, B, Chem.* **130**, 216–221 (2008)
- I.F. Cheng, H.C. Chang, D. Hou, H.C. Chang, An integrated dielectrophoretic chip for continuous bioparticle filtering, focusing, sorting, trapping, and detecting. *Biomicrofluidics* **1**, 15 (2007)
- S. Choi, J.K. Park, Continuous hydrophoretic separation and sizing of microparticles using slanted obstacles in a microchannel. *Lab Chip* **7**, 890–897 (2007)
- D.A. Colling, Intrinsic magnetization of Fe-Ni-Mn alloys. *J. Appl. Phys.* **40**, 1379–1381 (1969)
- K. Dholakia, M.P. MacDonald, P. Zemanek, T. Cizmar, Cellular and colloidal separation using optical forces. *Laser Manipulation of Cells and Tissues* **82**, 467–495 (2007)
- A. Ditsch, J. Yin, P.E. Laibinis, D.I.C. Wang, T.A. Hatton, Ion-exchange purification of proteins using magnetic nanoclusters. *Biotechnol. Prog.* **22**, 1153–1162 (2006)
- A.D. Ebner, J.A. Ritter, L. Nunez, High-gradient magnetic separation for the treatment of high-level radioactive wastes. *Sep. Sci. Technol.* **34**, 1333–1350 (1999)
- A.B. Frazier, Metallic microstructures fabricated using photosensitive polyimide electroplating molds. *J. Microelectromech. Syst.* **2**, 87–94 (1993)
- P.R.C. Gascoyne, J. Vykoukal, Particle separation by dielectrophoresis. *Electrophoresis* **23**, 1973–1983 (2002)
- K.H. Han, A.B. Frazier, Continuous magnetophoretic separation of blood cells in microdevice format. *J. Appl. Phys.* **96**, 5797–5802 (2004)
- K.H. Han, A.B. Frazier, Diamagnetic capture mode magnetophoretic microseparator for blood cells. *J. Microelectromech. Syst.* **14**, 1422–1431 (2005a)
- K.H. Han, A.B. Frazier, Reliability aspects of packaging and integration technology for microfluidic systems. *IEEE Transactions on Device and Materials Reliability* **5**, 452–457 (2005b)

- K.H. Han, A.B. Frazier, Paramagnetic capture mode magnetophoretic microseparator for blood cells. *IEE Proc. Nanobiotechnol.* **153**, 67–73 (2006a)
- K.H. Han, A.B. Frazier, Paramagnetic capture mode magnetophoretic microseparator for high efficiency blood cell separations. *Lab Chip* **6**, 265–273 (2006b)
- K.H. Han, A.B. Frazier, Lateral-driven continuous dielectrophoretic microseparators for blood cells suspended in a highly conductive medium. *Lab Chip* **8**, 1079–1086 (2008)
- L.A. Herzenberg, D. Parks, B. Sahaf, O. Perez, M. Roederer, L.A. Herzenberg, The history and future of the fluorescence activated cell sorter and flow cytometry: A view from Stanford. *Clin. Chem.* **48**, 1819–1827 (2002)
- Y. Kakihara, T. Fukunishi, S. Takeda, S. Nishijima, A. Nakahira, Superconducting high gradient magnetic separation for purification of wastewater from paper factory. *IEEE Trans. Appl. Supercond.* **14**, 1565–1567 (2004)
- M.P. MacDonald, G.C. Spalding, K. Dholakia, Microfluidic sorting in an optical lattice. *Nature* **426**, 421–424 (2003)
- M.P. MacDonald, S. Neale, L. Paterson, A. Richies, K. Dholakia, G.C. Spalding, Cell cytometry with a light touch: Sorting microscopic matter with an optical lattice. *J. Biol. Regul. Homeost. Agents* **18**, 200–205 (2004)
- H. Maenaka, M. Yamada, M. Yasuda, M. Seki, Continuous and size-dependent sorting of emulsion droplets using hydrodynamics in pinched microchannels. *Langmuir* **24**, 4405–4410 (2008)
- D. Melville, F. Paul, S. Roath, High gradient magnetic separation of red-cells from whole-blood. *IEEE Trans. Magn.* **11**, 1701–1704 (1975)
- S. Miltenyi, W. Muller, W. Weichel, A. Radbruch, High-gradient magnetic cell-separation with MACS. *Cytometry* **11**, 231–238 (1990)
- G.D. Moeser, K.A. Roach, W.H. Green, P.E. Laibinis, T.A. Hatton, Water-based magnetic fluids as extractants for synthetic organic compounds. *Ind. Eng. Chem. Res.* **41**, 4739–4749 (2002)
- A.F. Ngomsik, A. Bee, M. Draye, G. Cote, V. Cabuil, Magnetic nano- and microparticles for metal removal and environmental applications: a review. *Comptes Rendus Chimie* **8**, 963–970 (2005)
- M. Ozkan, M. Wang, C. Ozkan, R. Flynn, A. Birkbeck, S. Esener, Optical manipulation of objects and biological cells in microfluidic devices. *Biomed. Microdevices* **5**, 61–67 (2003)
- N. Pamme, C. Wilhelm, Continuous sorting of magnetic cells via on-chip free-flow magnetophoresis. *Lab Chip* **6**, 974–980 (2006)
- N. Pamme, J.C.T. Eijkel, A. Manz, On-chip free-flow magnetophoresis: Separation and detection of mixtures of magnetic particles in continuous flow. *J. Magn. Magn. Mater.* **307**, 237–244 (2006)
- M.S. Pommer, Y.T. Zhang, N. Keerthi, D. Chen, J.A. Thomson, C.D. Meinhart, H.T. Soh, Dielectrophoretic separation of platelets from diluted whole blood in microfluidic channels. *Electrophoresis* **29**, 1213–1218 (2008)
- A.J. Richards, O.S. Roath, R.J.S. Smith, J.H.P. Watson, The mechanisms of high gradient magnetic separation of human blood and bone marrow. *IEEE Trans. Magn.* **32**, 459–470 (1996)
- J.A. Ritter, A.D. Ebner, K.D. Daniel, K.L. Stewart, Application of high gradient magnetic separation principles to magnetic drug targeting. *J. Magn. Magn. Mater.* **280**, 184–201 (2004)
- M. Sarikaya, T. Abbasov, M. Erdemoglu, Some aspects of magnetic filtration theory for removal of fine particles from aqueous suspensions. *J. Dispers. Sci. Technol.* **27**, 193–198 (2006)
- T. Schneider, L.R. Moore, Y. Jing, S. Haam, P.S. Williams, A.J. Fleischman, S. Roy, J.J. Chalmers, M. Zborowski, Continuous flow magnetic cell fractionation based on antigen expression level. *J. Biochem. Biophys. Methods* **68**, 1–21 (2006)
- Y.Y. Sun, X.C. Yuan, L.S. Ong, J. Bu, S.W. Zhu, R. Liu, Large-scale optical traps on a chip for optical sorting. *Appl. Phys. Lett.* **90**, (2007)
- M. Takayasu, D.R. Kelland, J.V. Minervini, Continuous magnetic separation of blood components from whole blood. *IEEE Trans. Appl. Supercond.* **10**, 927–930 (2000)
- A. Thiel, A. Scheffold, A. Radbruch, Immunomagnetic cell sorting—pushing the limits. *Immunotechnology* **4**, 89–96 (1998)
- T.E. Thomas, S.J.R. Abraham, A.J. Otter, E.W. Blackmore, P.M. Lansdorp, High-gradient magnetic separation of cells on the basis of expression levels of cell-surface antigens. *J. Immunol. Methods* **154**, 245–252 (1992)
- M. Toner, D. Irimia, Blood-on-a-chip. *Annu. Rev. Biomed. Eng.* **7**, 77–103 (2005)
- S. Vankrunkelsven, D. Clicq, K. Pappaert, W. Ranson, C. De Tandt, H. Ottevaere, H. Thienpont, G.V. Baron, G. Desmet, A novel microstep device for the size separation of cells. *Electrophoresis* **25**, 1714–1722 (2004)
- M.M. Wang, E. Tu, D.E. Raymond, J.M. Yang, H.C. Zhang, N. Hagen, B. Dees, E.M. Mercer, A.H. Forster, I. Kariv, P.J. Marchand, W.F. Butler, Microfluidic sorting of mammalian cells by optical force switching. *Nat. Biotechnol.* **23**, 83–87 (2005)
- N. Xia, T.P. Hunt, B.T. Mayers, E. Alsberg, G.M. Whitesides, R.M. Westervelt, D.E. Ingber, Combined microfluidic-micromagnetic separation of living cells in continuous flow. *Biomed. Microdevices* **8**, 299–308 (2006)
- M. Yamada, M. Seki, Microfluidic particle sorter employing flow splitting and recombining. *Anal. Chem.* **78**, 1357–1362 (2006)
- B.B. Yellen, Z.G. Forbes, D.S. Halverson, G. Fridman, K.A. Barbee, M. Chorny, R. Levy, G. Friedman, Targeted drug delivery to magnetic implants for therapeutic applications. *J. Magn. Magn. Mater.* **293**, 647–654 (2005)
- M. Zborowski, G.R. Ostera, L.R. Moore, S. Milliron, J.J. Chalmers, A.N. Schechter, Red blood cell magnetophoresis. *Biophys. J.* **84**, 2638–2645 (2003)